Desalination and Water Treatment
www.deswater.com

doi: 10.5004/dwt.2020.26557

208 (2020) 434–447
December

Central composite design for the advanced treatment of biologically treated leachate nanofiltration concentrate using zero-valent copper and iron activated persulfate

Gamze Varank, Senem Yazici Guvenc*, Aleyna Çebi, Emine Can Güven

Department of Environmental Engineering, Yıldız Technical University, Davutpasa Campus, Esenler, Istanbul, 34220, Turkey, Tel. +90.212.3835383; Fax: +90.212.3835358; emails: syazici@yildiz.edu.tr, senem.yazici87@gmail.com (S.Y. Guvenc); Tel. +90.212.3835377; Fax: +90.212.3835358; email: gvarank@yildiz.edu.tr (G. Varank), Tel. +90.212.3835377; Fax: +90.212.3835358; email: aleyna94c@gmail.com (A. Cebi), Tel. +90 212 383 5428; Fax: +90 212 383 5358; email: ecguven@yildiz.edu.tr (E.C. Guven)

Received 2 May 2020; Accepted 6 September 2020

ABSTRACT

The purpose of this study was to investigate chemical oxygen demand (COD) removal from leachate nanofiltration concentrate with high resistant organic matter content by persulfate (PS) oxidation in which zero-valent copper (ZVCu) and zero-valent iron (ZVI) are used as activators. Within the scope of the study, response surface methodology (RSM) was applied to determine the optimum operating conditions by which maximum COD removal efficiency would be obtained, and effects of independent variables (pH, PS concentration, dosage of ZVI and ZVCu, reaction time) on COD removal efficiency and their interaction with each other were determined. The degree of significance of each independent variable was determined by analysis of variance. Estimated COD removal efficiencies under optimum conditions determined by the model were found to be 36.48% and 47.15%, respectively, for ZVCu-activated PS (ZVCu/PS) and ZVI-activated PS (ZVI/PS) processes whereas experimental removal efficiencies were 34.29% and 45.56%, respectively, for ZVCu/PS and ZVI/PS processes. The results of the study indicated that ZVI and ZVCu activated PS oxidation is effective and economic for COD removal from leachate nanofiltration concentrate with the BOD_5/COD ratio of 0.042, and RSM is a suitable method for the design and optimization of both processes.

Keywords: Leachate nanofiltration concentrate; ZVCu; ZVI; Persulfate oxidation; CCD

1. Introduction

In developing countries, landfilling is the most suitable strategy for solid waste management [1]. In landfills, high amounts of leachate form as the result of the rain flow along the landfill body and the decomposition of the disposed organic wastes at the site [2]. Leachate is a complex structured wastewater with the content of organic matter and ammonium in high concentrations, heavy metals, and a wide variety of toxic compounds. Therefore, leachate characteristics do not meet the discharge limits of Turkey's Water Pollution Control Regulations' Standards after the application of conventional treatment techniques (aerobic, anaerobic, biological treatment). Membrane filtration following the conventional biological treatment is applied in Turkey as in many European countries for the leachates to meet strict discharge limits. Generally, pressure-driven membrane processes consisting of ultrafiltration and nanofiltration are preferred for the membrane filtration. These processes have advantages as easy operation, lack of chemical additives, and low energy requirements [3]. However, as a result of these processes, membrane concentrates containing a high amount of resistant organic matter

* Corresponding author.

(humic substance, aromatic, and chlorinated compounds), and salt compounds are formed [4]. The membrane concentrates constitute about 13%–30% of the initial leachate volume. Dominant fractions of the dissolved organic matter, present in the content of membrane concentrates, are hydrophilic organic matter and humic substances with low biodegradability [2,5,6]. The high concentrations of resistant organic content and salt compounds cause low biodegradability. Various wastewater treatment processes such as recirculation, membrane distillation, evaporation, adsorption, coagulation, and advanced oxidation processes are applied in the treatment of membrane concentrates [4,7–12].

Advanced oxidation processes are effective methods in the decomposition of numerous organic matters in leachate. Pollutant removal is ensured through decomposition processes in advanced oxidation processes while it is based on phase change in other wastewater treatment methods such as physicochemical or separation methods [13]. One of the most extensively used advanced oxidation processes is the Fenton process by reasons such as not having high operating cost, and not requiring large scales means. Even if the Fenton process ensures high efficiency, factors such as the requirement of acidic conditions, high sludge formation, slow regeneration of iron ions, and requirement of a high amount of chemicals are limiting the field of application of the process [14,15].

Therefore, alternative oxidation technologies have gained importance. In-situ chemical oxidation is one of the promising technologies in wastewater treatment as it ensures rapid organic matter decomposition by the radicals generated during the processes [16–19]. The most extensively used oxidizing agents at in-situ chemical oxidation are ozone (O_3), hydrogen peroxide (H_2O_2), and permanganate. Recently, the use of persulfate as another oxidizing agent is becoming widespread due to its stability and high oxidation potential (2.01 V). Persulfate is an alternative oxidant ensuring the formation of radicals having high redox potential as hydroxyl radical (2.0–2.8 V) and sulfate radical (2.5–3.1 V) [20]. Persulfate is a thermodynamically strong oxidant with two electrons, but its direct reaction with most of the reductors is slow. Sulfate radicals (2.6 V), which are stronger oxidants than the persulfate anion, are formed due to the activation of persulfate. Sulfate radicals are generated as the result of hemolytic decomposition of peroxide bond in persulfate or peroxymonopersulfate [21]. The activation capacity of peroxymonopersulfate is higher compared with persulfate due to its asymmetric structure; however, PS is more preferred in the applications due to its properties such as being low cost and having high stability [22,23].

The sulfate radicals then initiate the formation of hydroxyl radicals (2.7 V) of higher redox potential and lower selectivity [24–26]. The lifetime of sulfate radicals is longer than that of hydroxyl radicals. The reason for this can be explained as the selective behavior of the sulfate radicals against the electron transfer reactions compared with hydroxyl radicals [27].

$$S_2O_8^{2-} \xrightarrow{hv/heat} 2SO_4^{-\bullet} \quad (1)$$

$$S_2O_8^{2-} + M^{n+} \rightarrow SO_4^{2-} + SO_4^{-\bullet} + M^{(n+1)+} \quad (2)$$

$$SO_4^{-\bullet} + OH^- \rightarrow SO_4^{2-} + {}^{\bullet}OH \quad (3)$$

$$SO_4^{-\bullet} + H_2O \rightarrow SO_4^{2-} + {}^{\bullet}OH + H^+ \quad (4)$$

Various methods are used for activating persulfate to form free radicals. These activation methods are chemical [24], light [28], ultrasound [29], electrochemical [30,31], and thermal methods [16]. Recently, transition metal ions have also been used for the activation of persulfate though it has been observed that not all the transition metals provide the expected activation efficiency.

Among the transition metals used for PS activation, the iron ion (Fe^{2+}) is one of the most effective methods commonly used due to the low cost, abundance, non-toxicity, and environmental friendly properties of the Fe^{2+} activation method [25]. The formation of sulfate radicals from persulfate through Fe^{2+} activation is provided by the following reactions [32].

$$Fe^{2+} + S_2O_8^{2-} \rightarrow SO_4^{\bullet-} + Fe^{3+} + SO_4^{2-} \quad (5)$$

$$Fe^{2+} + SO_4^{\bullet-} \rightarrow Fe^{3+}SO_4^{2-} \quad (6)$$

Since sulfate radical generation by the reaction of Fe^{2+} aqueous solution and persulfate occurs at a very high speed, it is very hard to control the mechanism. Also, excessive Fe^{2+} present in the solution reacts with the sulfate radicals and decreases both the amount and effectiveness of the sulfate radicals. A high concentration of Fe^{2+} is required for persulfate activation since Fe^{2+} is regenerated slowly after the conversion of Fe^{2+} to Fe^{3+}. This causes sulfate radical scavenging by Fe^{2+}, and thereafter pollutant removal efficiency through the persulfate oxidation decreases. Besides, Fe^{2+} and Fe^{3+} precipitate over the pH value of 5. Fe^{2+} control should be ensured for the effective utilization of persulfate. Another transition metal, used as an activator in persulfate oxidation in which the reactive radicals form, is copper. Copper typically exists in the form of Cu(I) or Cu(II). The potential of Cu(II) to oxidize persulfate is low, and Cu(I) is not stable and it cannot dissolve easily.

Recently, instead of homogenous activators [33,34], heterogeneous activators such as Fe minerals, iron oxide, nanoscale zero-valent iron (ZVI), nanoscale zero-valent copper are used by the researchers for the persulfate activation [35]. Fe^{2+} or Cu^+ is released into the solution by corrosion of zero-valent metals [36,37], and the dissolution process occurs slowly [34]. Through the use of ZVI for persulfate activation, not only the consumption of sulfate radicals by the excessive Fe^{2+} is prevented but also the introduction of other anions such as chloride and sulfate is also prevented.

Persulfate activation by ZVI has been defined by the following equations.

$$Fe^0 \rightarrow Fe^{2+} + 2e^- \quad (7)$$

$$2Fe^0 + O_2 + 2H_2O \rightarrow 2Fe^{2+} + 4^-OH \quad (8)$$

$$Fe^0 + S_2O_8^{2-} \rightarrow Fe^{2+} + SO_4^{2-} \quad (9)$$

$$Fe^0 + 2S_2O_8^{2-} \rightarrow 2SO_4^{\bullet-} + Fe^{2+} + 2SO_4^{2-} \quad (10)$$

Fe^{2+} releases from the corrosion of ZVI similarly Cu^+ is released as a result of the corrosion of zero-valent copper. The route followed in the release of Cu^+ through the corrosion of zero-valent copper is as follows: primarily Cu^+ continuously dissolves through the acid corrosion (Eq. (11)). In the second step, as similar to the Haber–Weiss mechanism in the Fenton-like process, Cu^+ forms during electron transfer from zero-valent copper to persulfate (Eq. (12)) [38]. In the third step, Cu^+ forms as the result of corrosion under anaerobic (Eq. (13)) or aerobic (Eqs. (14) and (15)) conditions [26]. Cu^+ formation accelerates through a reaction in between Cu^+ and persulfate because Cu^+ is the activator for persulfate decomposition. Zero-valent copper and Cu^+ cause H_2O_2 formation by reducing the molecular oxygen (Eqs. (15) and (16)) [23,26,39], and then hydroxyl radical forms as the result of activation of H_2O_2 by Cu^+ (Eq. (17)).

$$2Cu^0 + 2H^+ \rightarrow 2Cu^+ + H_2 \quad (11)$$

$$2Cu^0 + S_2O_8^{2-} \rightarrow 2Cu^+ + 2SO_4^{2-} \quad (12)$$

$$2Cu^0 + 2H_2O + 2Cu^+ + 2OH^- + H_2 \quad (13)$$

$$4Cu^0 + O_2 + 2H_2O \rightarrow 4Cu^+ + 4OH^- \quad (14)$$

$$2Cu^0 + O_2 + 2H_2O \rightarrow 2Cu^+ + H_2O_2 + 2OH^- \quad (15)$$

$$Cu^+ + O_2 + 2H^+ \rightarrow Cu^{2+} + H_2O_2 \quad (16)$$

$$Cu^+ + H_2O_2 \rightarrow Cu^{2+} + {}^{\bullet}OH + OH^- \quad (17)$$

There have been numerous studies investigating the removal of resistant pollutants with low biodegradability through advanced treatment processes in which sulfate radicals were generated by persulfate activation by various methods in literature [40–42]. On the other hand, recently sulfate radical–based advanced oxidation processes (SR-AOPs) have been applied for leachate treatment [15,43–46]. Although successful studies related to leachate treatment or resistant organic matter removal by SR-AOPs exist in the literature, to the best of our knowledge, a work studying the treatment of nanofiltration concentrate of biologically stabilized leachate through oxidation of persulfate activated by ZVCu and ZVI is deficient. The present work differs from other studies by the use of ZVCu and ZVI for persulfate activation in leachate concentrate treatment including high concentrations of recalcitrant organic matter. In this study, chemical oxygen demand (COD) removal from leachate nanofiltration concentrate through oxidation of persulfate, activated by Fe^{2+} and Cu^+ arising from ZVI and zero-valent copper corrosion processes was investigated. Response surface methodology and central composite design (CCD) were applied for experimental and statistical evaluation of the parameters being effective on the process and optimization of the independent process variables.

2. Materials and methods

2.1. Concentrated leachate characteristics

Leachate nanofiltration concentrate samples were obtained from the effluent of the nanofiltration unit of Leachate Treatment Plant located at Istanbul–Kömürcüoda Sanitary Landfill where 4,500 tons of solid waste disposed of per day. The flow scheme of Kömürcüoda Leachate Treatment Plant is given in Fig. 1. The samples were stored at the laboratory at 4°C in the dark and preserved as per standard methods to prevent biological activation. The characterizations of the influent and effluent leachate nanofiltration concentrate are shown in Table 1.

2.2. Chemicals

Potassium persulfate ($K_2S_2O_8$) (purity 99%) was purchased from Merck Company (ACS, ISO, Reag. Ph Eur quality, Turkey), zero-valent copper (Cu) and iron (Fe) were obtained from Sigma–Aldrich (Turkey). All chemicals were used as received without further purification. The pH of the wastewater in each run was adjusted using H_2SO_4 and NaOH solutions.

2.3. Experimental study and design

The experiments were carried out at room temperature in glass beakers on the jar-test device using a 250 mL sample. Experimental conditions determined by the CCD matrix (initial pH: 2–6, PS concentration: 5–45 mM, ZVCu or ZVI dosage: 1.5–7.5 g/L, and reaction time: 20–180 min) are given in Table 2. Before each experimental set, the pH level was adjusted to the required level by the use of H_2SO_4 or NaOH after persulfate addition. Then, the beakers were placed on the jar-test device, and reactions were initiated by adding determined amounts of ZVCu or ZVI. Rapid stirring for 2 min at 200 rpm was applied for the homogenous distribution of the chemicals. After rapid stirring, slow stirring at 30 rpm was applied for a period determined as per the experimental design matrix. At the end of the reaction time, the pH of each experimental set was adjusted over the value of 8 by the use of 6 N NaOH to improve the precipitation quality of flocks, and each experimental set was left for an hour for the precipitation of flocks. COD analyses were performed on supernatant samples to assess the performance of the process and the results were optimized by the use of CCD.

In experimental studies, it is important to reveal the interaction between the independent variables (X_1, X_2, ….. X_n) and responses (Y_1, Y_2, …Y_n). Various optimization methods are used to determine this relationship. In traditional multifactor optimization, the variation of a single factor is studied by keeping the other factors constant. This approach is called as one-factor at a time approach and it causes time loss while the interaction among the factors is unable to be evaluated. Consequently, it is not possible to obtain accurate optimum conditions by this method. Response surface methodology (RSM), which is an experimental design, was applied for obtaining the optimum results with high accuracy.

RSM is a statistical method that uses obtained quantitative data in the experimental study for solving the multi-variant equations. The main purpose of RSM is to obtain the

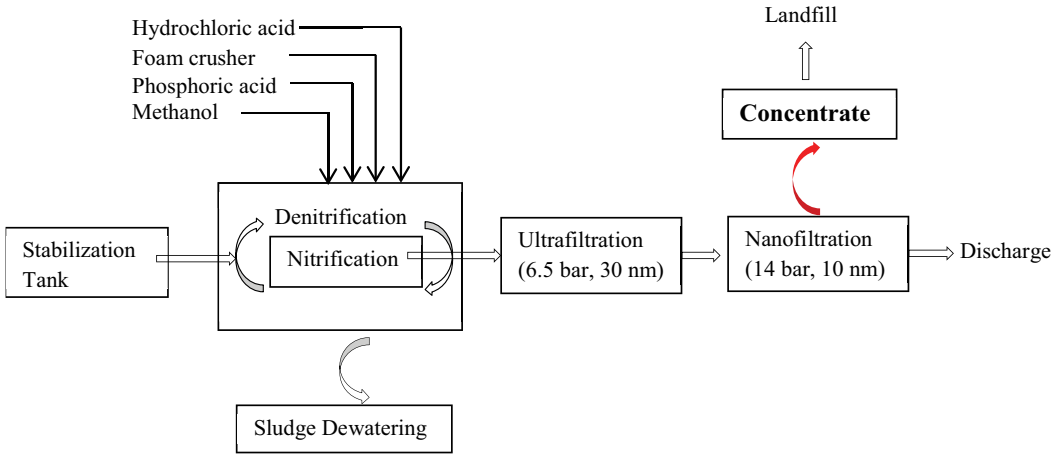

Fig. 1. Kömürcüoda Leachate Treatment Plant flow scheme.

Table 1
Characterizations of the influent and effluent leachate nanofiltration concentrate

Parameter	Influent	Effluent of the ZVI/PS process	Effluent of the ZVCu/PS process
pH	7.43	2.62	2.76
Conductivity, mS/cm	22.4	15.3	17.9
COD, mg/L	6,500	3,526	4,221
BOD_5, mg/L	273	220	235
BOD_5/COD	0.042	0.062	0.056
TSS, mg/L	35	20	23
Chloride, mg/L	7,035	5,320	5,980

Table 2
Independent variables and their coded levels

Symbol	Factor	Coded levels				
		–2	–1	0	+1	+2
A	pH	2	3	4	5	6
B	PS concentration, mM	5	15	25	35	45
C	ZVCu or ZVI dosage, g/L	1.5	3	4.5	6	7.5
D	Reaction time, min	20	60	100	140	180

optimal response. There are various RSM techniques including CCD [47], Box–Behnken statistical experiment design [48], and two-level full factorial design [49] used by the researchers for estimating the final optimum response.

CCD, revealed by Box and Wilson in 1951, is still the most popular method of RSM. CCD consists of three steps; performing the designed experimental study, estimating the coefficients of the mathematical model, predicting the responses, and the variation of the model. CCD requires a minimum number of sets consisting of standard 2^n factorials at the origin point at the center, $2n$ points fixed as axially at the alpha distance, and repetition tests at the center [50].

To completely reveal the relationship between the responses and the variables, a function in the form of $y = f(X_1, X_2,\ldots,X_n+\varepsilon)$ is determined (f represents the unknown response surface). Here, Y represents the response, X represents the independent variables, n represents the number of factors, and ε represents the experimental error. CCD-based RSM operates over the coded values of process' variables. The relationship between the real values and coded form of process' variables is expressed by the following equation.

$$\text{Coded value} = x_i = \frac{X_i - X_{\text{avg}}}{\Delta X} \tag{18}$$

X_i is the real value of the ith factor, X_{avg} is the average of lowest and highest values of ith factor, and ΔX is the step change. To obtain the correct functional relationship between the independent variables and the response, a second-degree polynomial equation is used. With the help of the equation, linear, quadratic, and interactive effects of the variables on the response can be defined.

This function is generally a first or second-degree polynomial function, and it is called as response surface method.

First-degree model:

$$y = \beta_0 + \sum_{i=1}^{n}\beta_i X_i + \varepsilon \tag{19}$$

Second-degree model:

$$Y = \beta_0 + \sum_{i=1}^{n}\beta_i X_i + \sum_{i=1}^{n}\beta_{ii}X_i^2 + \sum_{i=1}^{n}\sum_{i=1}^{i<j}\beta_{ij}X_iX_j + \varepsilon \quad (20)$$

where β_i, β_{ii}, β_{ij}, i, j, n indicate regression coefficients. While the first-degree model is defining a linear surface, the second-degree model defines a curved surface covering all the first and second-degree terms and their interactions. The second-degree model is called as quadratic model and reveals a good estimation for RSM.

In this study, the design of experimental results, data analysis, and optimization of independent variables of the process were performed by the use of CCD and response surface method. The equation of the quadratic model estimating the relationship between the dependent response variables and independent variables is as follows:

$$y = \beta_0 + \beta_1x_1 + \beta_2x_2 + \beta_3x_3 + \beta_4x_4 + \beta_{11}x_1^2 + \beta_{22}x_2^2 + \beta_{33}x_3^2 + \beta_{44}x_4^2 + \beta_{12}x_1x_2 + \beta_{13}x_1x_3 + \beta_{14}x_1x_4 + \beta_{23}x_2x_3 + \beta_{24}x_2x_4 + \beta_{34}x_3x_4 \quad (21)$$

where y is the model's response value (COD removal efficiency, %), x_1, x_2, x_3, x_4 are the level of independent variables (pH, PS, concentration, the dosage of ZVCu or ZVI, and reaction time), β_0 is the constant coefficient, β_1, β_2, β_3, β_4 are the linear regression coefficients β_{11}, β_{22}, β_{33}, β_{44} are the quadratic regression coefficients, and β_{12}, β_{13}, β_{14}, β_{23}, β_{24}, β_{34} are the interactive regression coefficients.

In this study, four variables of the process consisting of pH, PS concentration, the dosage of ZVI and ZVCu, and reaction time were studied by CCD using the Design Expert 11.0.1.0 software program. It is also important to check the adequacy of the conformity of the developed model. Analysis of variance (ANOVA) was applied for defining the significant parameters and determining the individual and interactive effects of these parameters on the COD removal efficiency. The significance of the process' variables was checked by the *p*-value and *F* value. 3 dimensional (3-D) graphs were drawn to reveal the interaction between the variables of the process.

2.4. Analytical methods

COD, BOD_5 and TSS analyses of leachate nanofiltration concentrate were conducted as per standard method 5220 C, 5210 B, 2540-D, respectively [51]. Color measurement was conducted using WTW Photolab 6600 spectrophotometer. pH and conductivity measurements were performed by the use of the WTW Multi 9620 IDS device.

COD removal efficiencies were calculated according to the following equation;

$$Y(\%) = \frac{C_i - C_f}{C_i} \times 100 \quad (22)$$

where Y is the removal efficiency (%), C_i is the initial COD concentration (mg/L) and C_f is the final COD concentration after the treatment processes.

Another significant parameter in the evaluation of process' performance in wastewater treatment applications is the operating cost. The treatment process to be applied should be preferred depending on both the contaminant removal efficiency and the process cost. Within this frame, the cost of ZVCu or ZVI-activated persulfate processes applied in this study was calculated by the following equation.

$$OC = \frac{(ZVM \times p) + (PS \times p)}{V \times (C_0 - C_{opt})} \quad (23)$$

where OC is the operating cost per removed pollutant amount (€/g removed *Y*), ZVM is the amount of zero-valent metal (ZVCu or ZVI, g) consumed, PS is the amount of persulfate consumed (g), p is the commercial market price of the chemical (US$/kg), V is the volume of wastewater (mL), C_0 is the initial pollutant concentration (mg/L), and C_{opt} is the pollutant concentration (mg/L) under optimum conditions.

3. Results and discussion

3.1. Statistical analysis and ANOVA results

Experimental results allow the development of mathematical equations to assess each *Y* response variable as a function of initial pH value, PS concentration, zero-valent metal amount, and reaction time. To determine the response variable by summing up the constant coefficient, four first degree effects (*A*, *B*, *C*, and *D*), six interactive effects (*AB*, *AC*, *AD*, *BC*, *BD*, and *CD*), and four quadratic effects (A^2, B^2, C^2, and D^2) were given in Eq. (21). The obtained results were analyzed by ANOVA and statistical parameters obtained by ANOVA for the two regression models are given in Table 3. It can be seen from Table 3 that *F* values of both models were determined to be high, that probability values (*p*-values) were determined to be less than 0.05, and that lack of fit values were determined to be higher than 0.05 [52]. This means that the models are statistically significant. *F* values determined as 32.59 and 18.52 for the ZVCu and ZVI processes, respectively, and *p* values determined as less than 0.0001 reveal that the obtained results are highly significant and that the relationship between the variables and responses for COD removal is explainable by the model. According to the results of ANOVA, it can be concluded that individual parameters of the process are more significant compared with combined parameters. As the *p*-values of all the linear parameters were found to be low in ZVCu and ZVI processes, it can be said that the parameter whose *F* value is higher is more significant. The parameters, which are expressed as more significant when compared with the others, are persulfate concentration and reaction time for the ZVCu/PS process whereas they are persulfate concentration and pH value for the ZVI/PS process. Only pH value from among quadratic parameters is significant for the ZVC/PS process, and only reaction time is significant for the ZVI/PS process. When the interactive parameters are considered, persulfate concentration × reaction time was determined as significant for the ZVC/PS process while the interactive parameters of persulfate concentration × zero-valent

Table 3
ANOVA results for ZVCu/PS and ZVI/PS processes

	ZVCu/PS						ZVI/PS					
	SS	df	MS	*F*-value	*p*-value	Remark	SS	df	MS	*F*-value	*p*-value	Remark
Model	1,488.20	14	106.30	18.52	<0.0001	HS	1722.12	14	123.01	32.59	<0.0001	HS
A-pH	292.67	1	292.67	50.98	<0.0001	HS	484.20	1	484.20	128.28	<0.0001	HS
B-PS. mM	521.27	1	521.27	90.80	<0.0001	HS	520.80	1	520.80	137.98	<0.0001	HS
C-ZVM, g/L	56.27	1	56.27	9.80	0.0087	S	229.40	1	229.40	60.78	<0.0001	HS
D-Time, min	413.09	1	413.09	71.95	<0.0001	HS	302.46	1	302.46	80.13	<0.0001	HS
AB	6.19	1	6.19	1.08	0.3197	NS	10.89	1	10.89	2.89	0.1152	NS
AC	0.8883	1	0.8883	0.1547	0.7010	NS	9.92	1	9.92	2.63	0.1309	NS
AD	2.60	1	2.60	0.4529	0.5137	NS	1.32	1	1.32	0.3504	0.5649	NS
BC	1.49	1	1.49	0.2603	0.6192	NS	29.70	1	29.70	7.87	0.0159	S
BD	50.66	1	50.66	8.82	0.0117	S	33.06	1	33.06	8.76	0.0119	S
CD	9.84	1	9.84	1.71	0.2149	NS	28.09	1	28.09	7.44	0.0183	S
A^2	105.27	1	105.27	18.34	0.0011	S	1.95	1	1.95	0.5158	0.4864	NS
B^2	1.61	1	1.61	0.2812	0.6056	NS	5.29	1	5.29	1.40	0.2594	NS
C^2	2.19	1	2.19	0.3808	0.5487	NS	16.72	1	16.72	4.43	0.0570	NS
D^2	2.07	1	2.07	0.3597	0.5598	NS	47.87	1	47.87	12.68	0.0039	S
Residual	68.89	12	5.74				45.29	12	3.77			
Lack of fit	67.43	10	6.74	9.19	0.1020	NS	44.45	10	4.44	10.50	0.0900	NS
Pure error	1.47	2	0.7336				0.8467	2	0.4233			
Cor. total	1557.09	26					1767.41	26				
R^2	0.9558						0.9744					
Adjusted R^2	0.9041						0.9445					
Predicted R^2	0.7485						0.8541					

metal dosage, persulfate concentration × reaction time, and zero-valent metal dosage × reaction time were found to be significant for the ZVI/PS process.

The coefficient of determination (R^2) expresses the explicability ratio of predictors covered by the model (X_s), and of the total variation in the response variable [53,54]. R^2 values were determined as 95.58% and 97.44% for ZVCu/PS and ZVI/PS processes, respectively. The high R^2 values express the conformity between the experimental data and estimated values [55]. COD removal variance is not explicable by the model by rates of 4.42%, and 2.56% in ZVC/PS and ZVI/PS processes, respectively. The coefficient of variation (CV) can be defined as the percentage ratio between the standard error of the estimated and the mean value of the observed response. CV value is a measure of the reproducibility feature of the model, and as a general rule, it is desired to be lower than 10% [54,56]. As the CV values of both models are lower than 10%, it can be said that the models are reasonably reproducible. Adequate precision is a measure of the range in predicted response relative to its associated error. It can also be defined as a signal-to-noise ratio. The value of adequate precision is desired to be at least 4 [57]. Adequate precision values of both models were found to be higher than the value of 4.

Conformity of the experimental data to a polynomial model representing the COD removal efficiency (%) (response *Y*), being a function of PS concentration, zero-valent metal dosage, initial pH value and reaction time, was analyzed by Design Expert 11.0.1.0 software program, and the equation of the model is given below.

For ZVCu/PS;

$$\text{COD removal} = +18.20 - 3.49A + 4.66B + 1.53C + 4.15D - 0.6219AB - 0.2356AC - 0.4031AD - 0.3056BC + 1.78BD - 0.7844CD + 2.22A^2 + 0.2751B^2 + 0.3201C^2 - 0.3111D^2 \quad (24)$$

For ZVI/PS;

$$\text{COD removal} = +28.13 - 4.49A + 4.66B + 3.09C + 3.55D - 0.8250AB - 0.7875AC - 0.2875AD - 1.36BC + 1.44BD - 1.33CD - 0.3021A^2 + 0.4979B^2 + 0.8854C^2 + 1.50D^2 \quad (25)$$

As can be seen from the equations that all linear parameters are more effective than the quadratic and interactive parameters in both processes, and linear effects of the parameters are higher than the quadratic effects of the same parameters. In other words, the increase in the values of the parameters is linearly increasing the COD removal efficiency [58]. Pareto graph analysis, where the linear, quadratic, and interactive effects of independent variables on the COD removal efficiency are shown, is given in Fig. 2 [59]. Among the linear parameters, the effect of the ZVCu and ZVI dosage is found to be lower compared with that of other

linear parameters. Persulfate concentration and reaction time have a synergic effect on the COD removal efficiency in both processes. The results obtained by the Pareto analysis conform to the results of ANOVA.

The graphs indicating the conformity of experimental values, and the predicted values provided by the regression equations obtained by the model are given in Fig. 3. The graphs give a first-degree line for both processes. R^2 values of graphs obtained for COD removal by ZVCu/PS and ZVI/PS processes were determined as 95.58% and 97.44%, respectively. High R^2 values indicate that the experimental data conform with the model's results. It was observed from both graphs that the estimated values obtained by the models were very close to the real values, and thus the validity of the equations was proven [60].

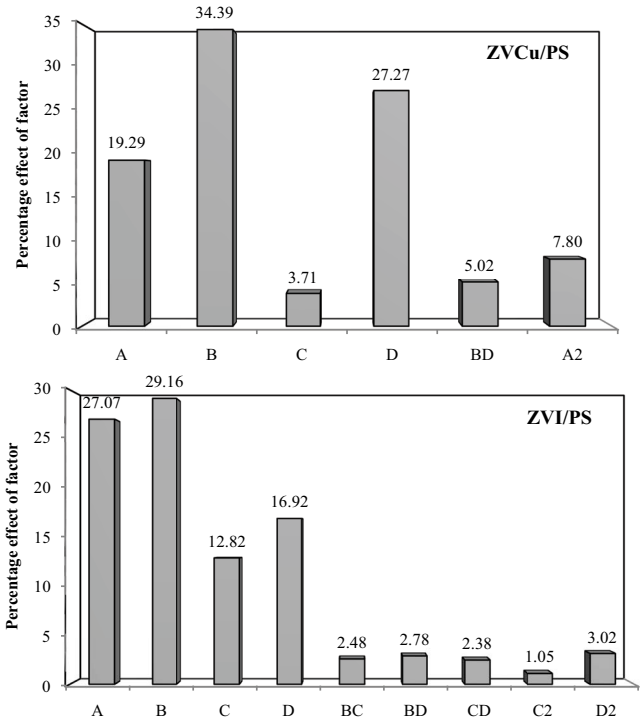

Fig. 2. Pareto curve for COD removal by ZVC/PS and ZVI/PS processes.

3.2. Effects of variables on COD removal

3D graphs, clearly indicating the effects of independent variables on the dependent variables, and their interaction with each other, are given in Figs. 4 and 5. It is being observed from the graphs that, in both processes, COD removal efficiency linearly increases as the PS concentration and zero-valent metal dosage increases. Again in both processes, COD removal efficiency increases as the reaction time increases, but the removal efficiency decreases as the pH value increases. Among the independent variables, the zero-valent metal dosage has the lowest effect. And also the effect of zero-valent copper on the process is found to be lower compared with that of ZVI.

pH value is one of the most critical factors affecting the system's performance in the decomposition of pollutants due to its function of controlling the activity of the free radicals and the catalytic activity. It is observed from Figs. 4 and 5 that in both processes COD removal efficiency decreases as pH increases. Acidic conditions are increasing the dispersion of Fe^{2+} from the surface of ZVI and mix in the solution. PS activation rate is also increasing depending on the increasing iron amount. ZVI corrodes in the presence of a high amount of protons, and Fe^{2+} released as the result of corrosion activates the persulfate, and sulfate radicals form. The highest COD removal efficiency was obtained as the pH value was at the range of 2–3, and COD removal efficiency decreased as the pH value gets close to neutral

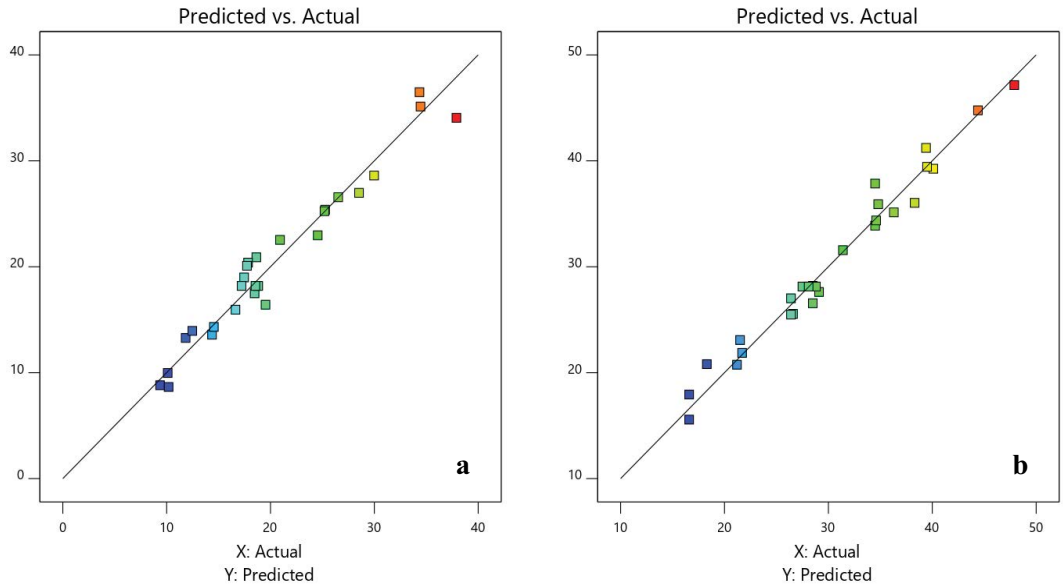

Fig. 3. Predicted vs. experimental COD removal (a): for ZVCu/PS and (b): for ZVI/PS processes.

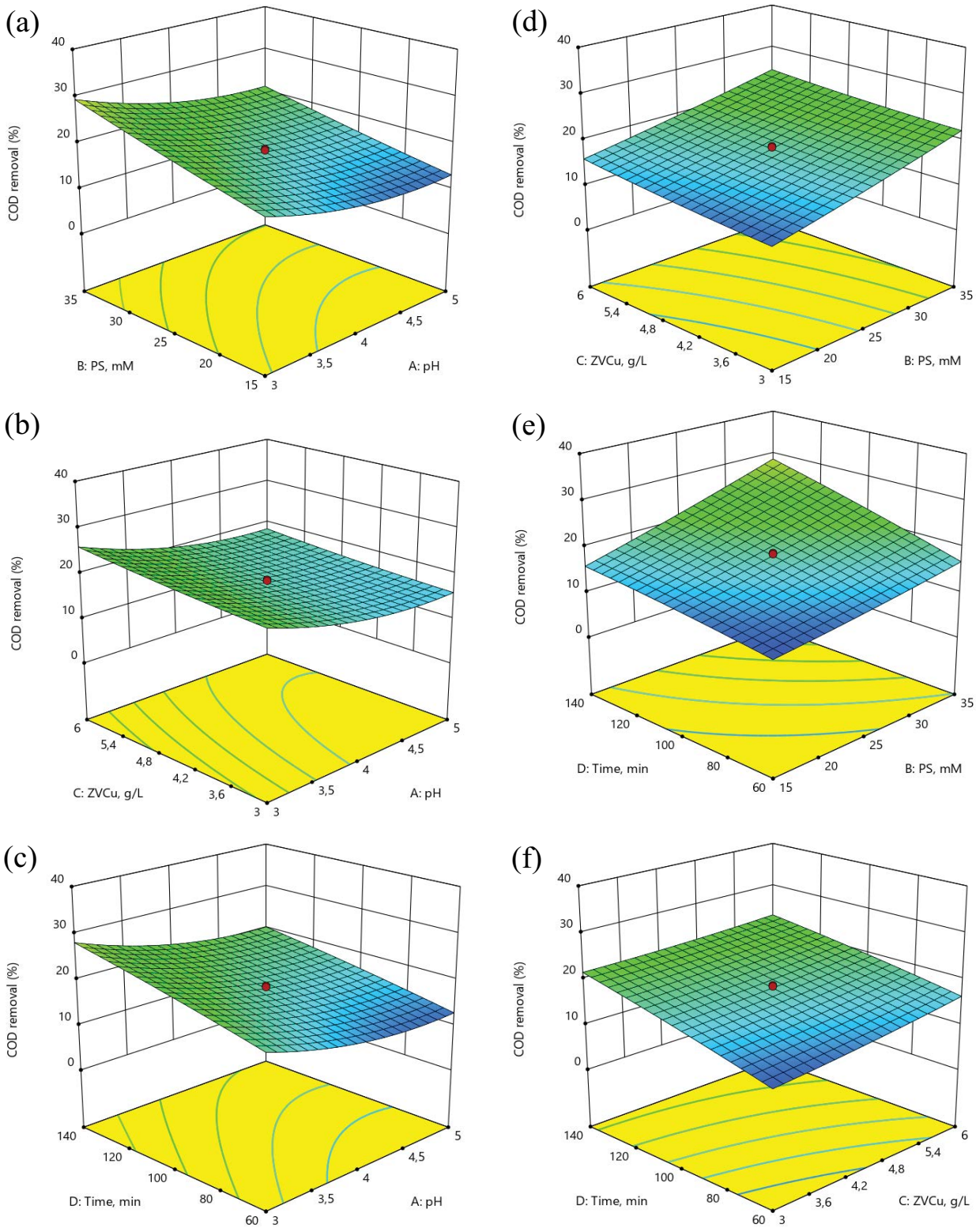

Fig. 4. 3-D plots surface of COD removal as a function: (a) pH and PS, (b) pH and ZVCu, (c) pH and time, (d) PS and ZVCu, (e) PS and time, (f) ZVCu and time for ZVCu/PS process.

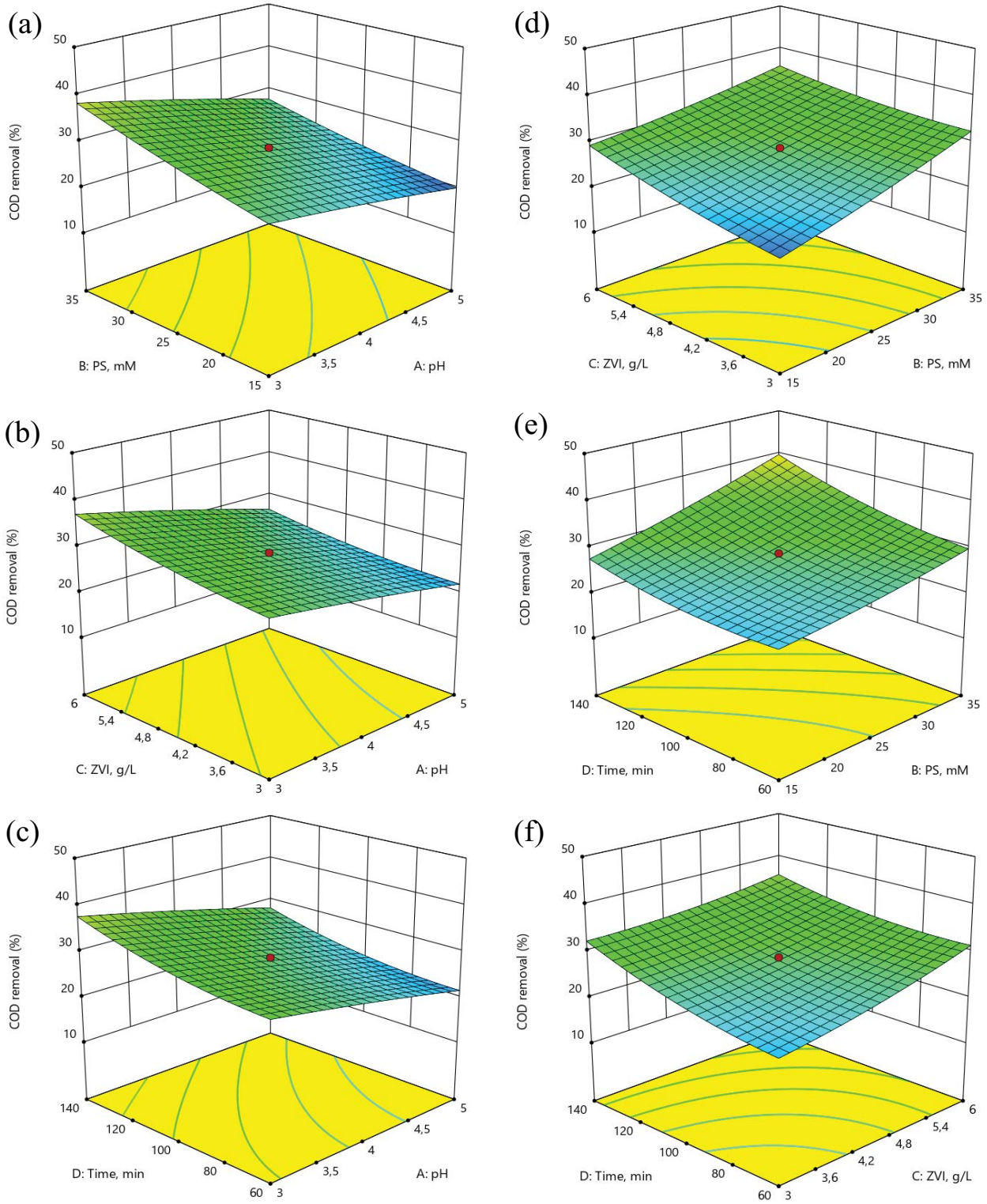

Fig. 5. 3-D plots surface of COD removal as a function: (a) pH and PS, (b) pH and ZVI, (c) pH and time, (d) PS and ZVI, (e) PS and time, (f) ZVI and time for ZVI/PS process.

values. The decreasing removal efficiency is relevant to the precipitation of iron types arising over pH 4. Iron hydroxide types deactivate the ZVI by precipitating in the form of $Fe(OH)_n$ and $Fe(OH)^{(n+1)+}$ [29,61,62]. Moreover, the strength of free radicals is higher under acidic conditions compared with alkali conditions [63]. For this reason, it can be concluded that the pH range of 2–3 is the most suitable pH range for both processes.

As the amount of zero-valent transition metal increases, Fe^{2+} and Cu^{+} concentration in the solution, as the result of corrosion, increases thus the amount of free radicals generated by persulfate activation also increases. Therefore, it can be said that COD removal efficiency increases as the dosage of ZVI and zero-valent copper increases. It is observed from Figs. 4 and 5 that, COD removal efficiency increases as the amount of ZVI and copper increases. The number of active sites increases as the dosage of zero-valent copper or iron increases, and thus release of a higher amount of copper and iron ion is observed as the result of corrosion. But this increase is not continuous. In the case of the addition of a high dosage of the zero-valent transition metal, excessive iron or copper ion reacts with the free radicals, and thereby amount of free radicals decreases [64]. As a result, the COD removal efficiency decreases. Since the range of the catalyst dosage selected in this study is not high, the scavenging effect of the excessive iron or copper ion on the sulfate and hydroxyl radicals and nonreactive anion formation was not observed.

$$Fe^{2+} + \left(SO_4^{\bullet -} \text{ or } HO^{\bullet}\right) \rightarrow Fe^{3+} + \left(SO_4^{2-} \text{or } OH^{-}\right) \quad (26)$$

Persulfate is the main source of sulfate and hydroxyl radicals. The increase in persulfate concentration will increase sulfate radical formation, and also increase the COD removal efficiency. Experimental studies showed that higher removal efficiencies were obtained as the persulfate concentration increases (Figs. 4 and 5). As similar to the catalyst dosage, excessive persulfate exhibits a behavior for scavenging the free radicals (sulfate and hydroxyl radicals). The studies in literature had reported that the target pollutant removal efficiency does not show a continuous increase as the persulfate dosage increases. In their study, Li et al. [65] had determined that when the persulfate concentration increases the amount of sulfate radical increases, and after reaching a specific amount, the radicals react with each other instead of reacting with the organic matter (Eq. (27)) [29,65]. Moreover, persulfate itself also serves as the destroyer of sulfate radicals (Eq. (28)) [66,67]. But as the persulfate concentration added in this study was under the inhibition point, the increase was observed in the COD removal efficiency as the persulfate concentration increases, but the decrease was not observed after a specific value.

$$SO_4^{\bullet -} + SO_4^{\bullet -} \rightarrow S_2O_8^{2-} \quad (27)$$

$$SO_4^{\bullet -} + S_2O_8^{2-} \rightarrow SO_4^{2-} + S_2O_8^{\bullet -} \quad (28)$$

To obtain maximum COD removal efficiency, optimum operating conditions were determined by numerical optimization technique using the software program in the determination of optimum process variables. Optimized conditions were determined as pH:3, PS concentration: 35 Mm, dosage of ZVI and ZVCu: 6 g/L, and reaction time: 140 min for both processes (Fig. 6). COD removal efficiencies predicted by the model under optimized conditions were determined to be 36.49% and 47.15% for ZVCu/PS and ZVI/PS processes, respectively. As a result of the experimental studies carried out, COD removal efficiencies obtained under optimum conditions were found as 34.29% and 45.56% for ZVCu/PS and ZVI/PS processes, respectively. These values indicate that the experimental and statistical data are in good agreement. Leachate nanofiltration concentrate with initial COD concentration of 6,500 mg/L, BOD_5 concentration of 273 mg/L, and the BOD_5/COD ratio of 0.042 was comprised of high inert COD content. COD concentration removed by the ZVCu/PS and ZVI/PS oxidation processes was determined as 2,278.9 and 2,974.4 mg/L, respectively, and it can be said that about half of the COD consisting of resistant organic matters were removed.

In operational cost analysis of oxidation processes, the costs of oxidant (persulfate) and activators (ZVCu or ZVI) are the most important issues. Under the optimum conditions, operational costs were calculated for both oxidation processes. The purchase costs of ZVCu, ZVI and $K_2S_2O_8$ with an analytical grade in Turkey's market (April 2020) are 111, 37 and 64 US$/kg, respectively. On this basis, the costs of the processes were calculated as 0.56 and 0.28 US$/g COD removed for ZVCu/PS and ZVI/PS, respectively. A comparison of the operational cost of sulfate radicals based advanced treatment processes is presented in Table 4. It can be concluded from Table 4 that the use of catalytic activators such as UV, micro-wave, H_2O_2 or electricity for accelerating the activation of the persulfate in wastewater treatment, not only increases pollutant removal efficiencies but also increases the operational costs. In the present study, ZVI/PS and ZVCu/PS processes are found to be economically feasible processes in the reduction of the pollution load of leachate nanofiltration concentrate and can be offered as a pre-treatment method.

4. Conclusion

RSM and four-factor five-level CCD was applied for COD removal from leachate nanofiltration concentrate through oxidation of persulfate in which ZVI and zero-valent copper were used as activators. By the application of CCD-based RSM, the effects of independent variables (pH, PS concentration, ZVCu and ZVI dosage, and reaction time) on the response (COD removal), and their interaction with each other were determined, and operational conditions were optimized for obtaining maximum COD removal efficiency. Under the optimum conditions determined by the model, statistically obtained COD removal efficiencies were determined as 36.49% and 47.15% for ZVCu/PS and ZVI/PS processes, respectively, whereas experimentally obtained COD removal efficiencies were determined as 34.29% and 45.56% for ZVCu/PS and ZVI/PS processes, respectively. The provision of high correlation coefficient values by the variance analysis indicates that the values estimated by the second-degree model, and experimental data conform to

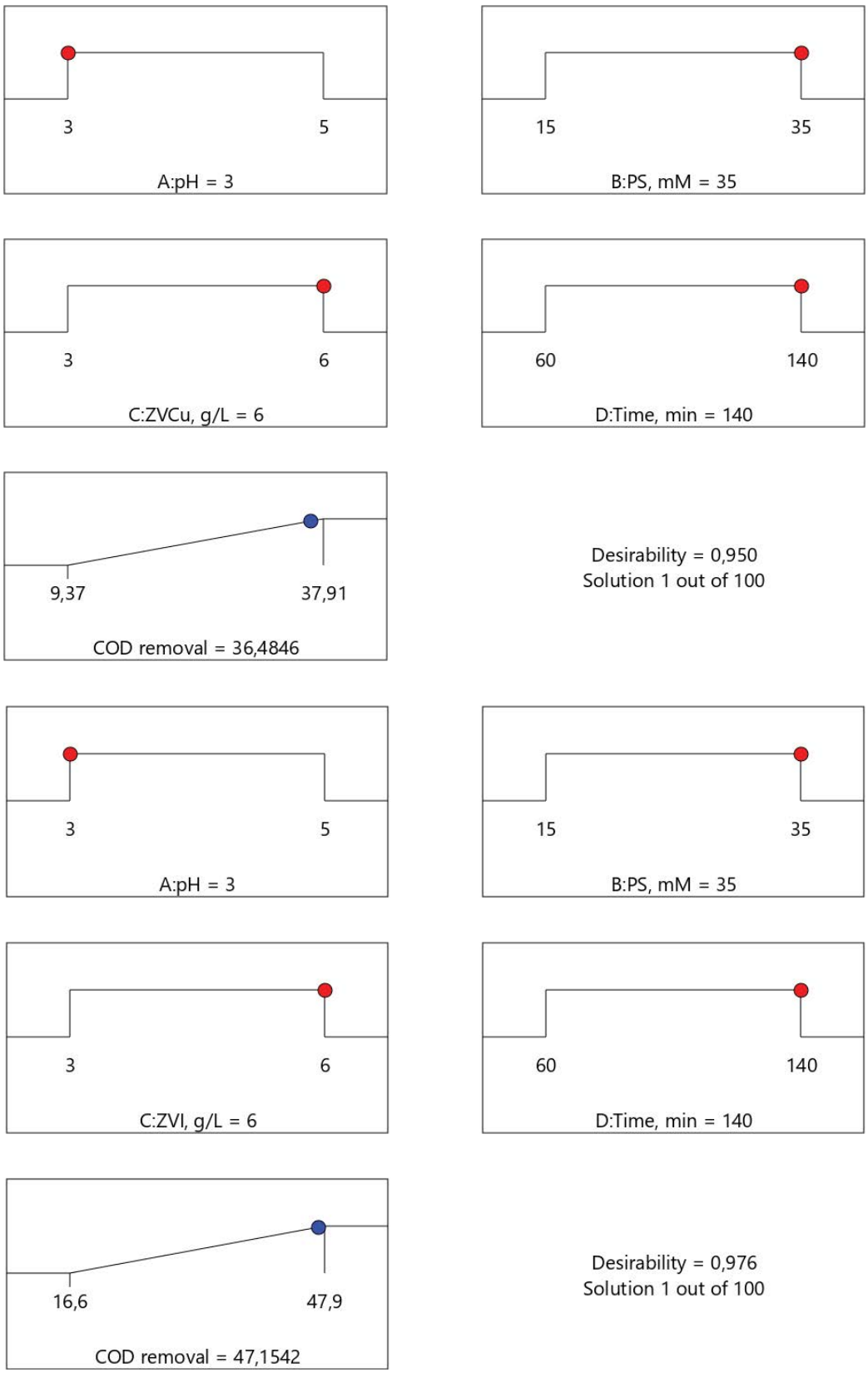

Fig. 6. Optimization conditions for maximum COD removal by ZVCu/PS process and ZVI/PS process.

Table 4
Comparison of the operational cost of sulfate radicals based advanced treatment processes

Reference	Type	Process	Pollutant removal, %	Operational cost
Present study	Leachate nanofiltration concentrate	ZVCu/PS ZVI/PS	COD: 34.29 COD: 45.56	0.56 US$/g COD 0.28 US$/g COD
[68]	Textile wastewater	PMS–ZVI PMS–ZVC H2O2–PMS–ZVI	COD:74.6 TOC: 48.1 COD:58.6 TOC: 39.3 COD:74.5 TOC: 50.8	1.16 US$/L g of removed COD 2.15 US$/L g of removed COD 0.71 US$/L g of removed COD
[69]	Petrochemical wastewater	UV/PS UV/PS/Fe^{2+}	COD: 66.3 COD: 74.5	22.96 (US$/ kg COD removed 24.52 (US$/ kg COD removed
[70]	Mineralization of unsymmetrical dimethylhydrazine	Persulfate activated by zero-valent iron nanoparticles	DOC: 91	10 US$/$m^3$
[71]	Mature landfill leachate	Microwave-enhanced persulfate oxidation	TOC: 79.4 Color: 88.4 UV_{254}: 77.1	USD$6.03/$m^3$
[72]	Degradation of direct red 16 (DR16)	UV/persulfate/Ce(IV)	DR16: 90	1.98 US$/$m^3$
[73]	Olive oil mill wastewater	Microwave-activated persulfate oxidation	TOC: 63.38 COD: 56.94 Color: 94.85	0.0633 Euro/g total organic carbon (TOC)
[74]	Concentrated leachate	Electro-persulfate	COD: 71.4	2.8 €/m^3
[75]	Leachate concentrate	Persulfate activation with microwave (MW) persulfate activation with conventional heating (CH)	COD removal of 53.3, color removal of 99.9 COD removal of 20, color removal of 65.4	25 €/L 16.5 €/L
[76]	Stabilized landfill leachate	$S_2O_8^{2-}/H_2O_2$	Organic matter: 81	10.73 USD/kg COD
[77]	Landfill leachate	Coagulation followed by MW-PS	COD: 89	72 $/kg COD removed

both processes. Depending on high *F* values, low *p*-values, and high lack of fit values obtained by ANOVA, it can be concluded that models are found to be significant for both processes studied. Consequently, ZVCu/PS and ZVI/PS processes give promising results for leachate nanofiltration treatment consisting of high inert COD content.

References

[1] R.K. Rowe, Y. Yu, Clogging of finger drain systems in msw landfills, Waste Manage., 32 (2012) 2342–2352.
[2] Y. Long, J. Xu, D. Shen, Y. Du, H. Feng, Effective removal of contaminants in landfill leachate membrane concentrates by coagulation, Chemosphere, 167 (2017) 512–519.
[3] H. Wang, X. Li, Z. Hao, Y. Sun, Y. Wang, W. Li, Y.F. Tsang, Transformation of dissolved organic matter in concentrated leachate from nanofiltration during ozone-based oxidation processes (O_3, O_3/ H_2O_2 and O_3/UV), J. Environ. Manage., 191 (2017) 244–251.
[4] R. He, B.H. Tian, Q.Q. Zhang, H.T. Zhang, Effect of Fenton oxidation on biodegradability, biotoxicity and dissolved organic matter distribution of concentrated landfill leachate derived from a membrane process, Waste Manage., 38 (2015) 232–239.
[5] Q.Q. Zhang, B.H. Tian, X. Zhang, A. Ghulam, C.R. Fang, R. He, Investigation on characteristics of leachate and concentrated leachate in three landfill leachate treatment plants, Waste Manage., 33 (2013) 2277–2286.
[6] B.O. Clarke, T. Anumol, M. Barlaz, S.A. Snyder, Investigating landfill leachate as a source of trace organic pollutants, Chemosphere, 127 (2015) 269–275.
[7] H. Zhang, D. Zhang, J. Zhou, Removal of COD from landfill leachate by electro-Fenton method, J. Hazard. Mater., 135 (2006) 106–111.
[8] Q. Liu, X. Zhang, Y. Zhou, A. Zhao, S. Chen, G. Qian, Z.P. Xu, Optimization of fermentative biohydrogen production by response surface methodology using fresh leachate as nutrient supplement, Bioresour. Technol., 102 (2011) 8661–8668.
[9] S.Y. Hunce, D. Akgul, G. Demir, B. Mertoglu, Solidification/ stabilization of landfill leachate concentrate using different aggregate materials, Waste Manage., 32 (2012) 1394–1400.
[10] X.Y. Li, L.W. Zhang, C.W. Wang, Review of disposal of concentrate streams from nanofiltration (NF) or reverse osmosis (RO) membrane process, Adv. Mater. Res., 518–523 (2012) 3470–3475.
[11] Q.Y. Wan, Y.L. Zhang, J.B. Lin, Catalyst activity on landfill leachate treatment with CWAO method, Appl. Mechanics Mater., 467 (2014) 127–132.

[12] X. Qi, C. Zhang, Y. Zhang, Treatment of Landfill Leachate RO Concentrate by VMD, International Conference on Circuits and Systems (CAS 2015).
[13] Y. Deng, J.D. Englehardt, Treatment of landfill leachate by the Fenton process, Water Res., 40 (2006) 3683–3694.
[14] Y. Deng, C.M. Ezyske, Sulfate radical-advanced oxidation process (SR-AOP) for simultaneous removal of refractory organic contaminants and ammonia in landfill leachate, Water Res., 45 (2011) 6189–6194.
[15] T.T. Asha, R. Gandhimathi, S.T. Ramesh, P.V. Nidheesh, Treatment of Stabilized Leachate by Ferrous-Activated Persulfate Oxidative System, J. Hazard. Toxic Radioact. Waste, 21 (2017) 04016012–1-6.
[16] A. Ghauch, A.M. Tuqan, N. Kibbi, Naproxen abatement by thermally activated persulfate in aqueous systems, Chem. Eng. J., 279 (2015) 861–873.
[17] B. Ranc, P. Faure, V. Croze, M.O. Simonnot, Selection of oxidant doses for in situ chemical oxidation of soils contaminated by polycyclic aromatic hydrocarbons (PAHs): a review, J. Hazard. Mater., 312 (2016) 280–297.
[18] S. Luo, L.W. Gao, Z.S. Wei, R. Spinney, D.D. Dionysiou, W.P. Hu, L.Y. Chai, R.Y. Xiao, Kinetic and mechanistic aspects of hydroxyl radical-mediated degradation of naproxen and reaction intermediates, Water Res., 137 (2018) 233–241.
[19] H. Chi, Z. Wang, X. He, J. Zhang, D. Wang, J. Ma, Activation of peroxymonosulfate system by copper-based catalyst for degradation of naproxen: mechanisms and pathways, Chemosphere, 228 (2019) 54–64.
[20] J. Wang, S. Wang, Activation of persulfate (PS) and peroxymonosulfate (PMS) and application for the degradation of emerging contaminants, Chem. Eng. J., 334 (2018) 1502–1517.
[21] L.J. Bu, S.M. Zhu, S.Q. Zhou, Degradation of atrazine by electrochemically activated persulfate using BDD anode: role of radicals and influencing factors, Chemosphere, 195 (2018) 236–244.
[22] D.H. Ding, C. Liu, Y.F. Ji, Q. Yang, L.L. Chen, C.L. Jiang, T.M. Cai, Mechanism insight of degradation of norfloxacin by magnetite nanoparticles activated persulfate: identification of radicals and degradation pathway, Chem. Eng. J., 308 (2017) 330–339.
[23] J. Deng, M. Xua, Y. Chena, J. Lic, C. Qiua, X. Lid, S. Zhoue, Highly-efficient removal of norfloxacin with nanoscale zero-valent copper activated persulfate at mild temperature, Chem. Eng. J., 366 (2019) 491–503.
[24] S.R. Rastogi, D.D. Ai-Abed, Dionysiou, Sulfate radical-based ferrous-peroxymonosulfate oxidative system for PCBs degradation in aqueous and sediment systems, Appl. Catal., B, Environ., 85 (2009) 171–179.
[25] P. Zhou, J. Zhang, J. Liu, Y. Zhang, J. Liang, Y. Liu, B. Liu, W. Zhang, Degradation of organic contaminants by activated persulfate using zero valent copper in acidic aqueous conditions, R. Soc. Chem. Adv., 6 (2016) 99532–99539.
[26] S.Q. Zhou, Y.H. Yu, J.L. Sun, S.M. Zhu, J. Deng, Oxidation of microcystin-LR by copper coupled with ascorbic acid: kinetic modeling towards generation of H_2O_2, Chem. Eng. J., 333 (2018) 443–450.
[27] C. Liang, C.J. Bruell, M.C. Marley, K.L. Sperry, Persulfate oxidation for in situ remediation of TCE. I. Activated by ferrous ion with and without a persulfate-thiosulfate redox couple, Chemosphere, 55 (2004) 1213–1223.
[28] Z. Xu, C. Shan, B. Xie, Y. Liu, B. Pan, Decomplexation of Cu(II)- EDTA by UV/persulfate and UV/H_2O_2: efficiency and mechanism, Appl. Catal., B, 200 (2017) 439–447.
[29] G. Barzegar, S. Jorfi, V. Zarezade, M. Khatebasreh, F. Mehdipour, F. Ghanbari, 4-Chlorophenol degradation using ultrasound/peroxymonosulfate/nanoscale zero valent iron: reusability, identification of degradation intermediates and potential application for real wastewater, Chemosphere, 201 (2018) 370–379.
[30] L. Chen, C. Lei, Z. Li, B. Yang, X. Zhang, L. Lei, Electrochemical activation of sulfate by BDD anode in basic medium for efficient removal of organic pollutants, Chemosphere, 210 (2018) 516–523.
[31] H. Song, L. Yan, J. Jiang, J. Ma, S. Pang, X. Zhai, W. Zhang, D. Li, Enhanced degradation of antibiotic sulfamethoxazole by electrochemical activation of PDS using carbon anodes, Chem. Eng. J., 344 (2018) 12–20.
[32] H. Liu, T.A. Bruton, W. Li, J.V. Buren, C. Prasse, F.M. Doyle, D.L. Sedlak, Oxidation of benzene by persulfate in the presence of Fe(III)- and Mn(IV)- containing oxides: stoichiometric efficiency and transformation products, Environ. Sci. Technol., 50 (2016) 890–898.
[33] I. Hussain, Y. Zhang, S. Huang, X. Du, Degradation of p-chloroaniline bypersulfate activated with zero-valent iron, Chem. Eng. J., 203 (2012) 269–276.
[34] X.L. Zou, T. Zhou, J. Mao, X.H. Wu, Synergistic degradation of antibioticsulfadiazine in a heterogeneous ultrasound-enhanced Fe^0/persulfate Fenton-like system, Chem. Eng. J., 257 (2014) 36–44.
[35] G.D. Fang, D.D. Dionysiou, S.R. Al-Abed, D.M. Zhou, Superoxide radical driving the activation of persulfate by magnetite nanoparticles: implications for the degradation of PCBs, Appl. Catal., B, 129 (2013) 325–332.
[36] Y. Segura, F. Martinez, J.A. Melero, J.L.G. Fierro, Zero valent iron (ZVI) mediated Fenton degradation of industrial wastewater: treatment performance and characterization of final composites, Chem. Eng. J., 269 (2015) 298–305.
[37] X. Zhou, W. Jin, H. Chen, C. Chen, S. Han, R. Tu, W. Wei, S.H. Gao, G.J. Xie, Q. Wang, Enhancing dewaterability of waste activated sludge by combined oxidative conditioning process with zero-valent iron and peroxymonosulfate, Water Sci. Technol., 76 (2017) 2427–2433.
[38] X.Y. Ma, Y.Q. Cheng, Y.J. Ge, H.D. Wu, Q.S. Li, N.Y. Gao, J. Deng, Ultrasound enhanced nanosized zero-valent copper activation of hydrogen peroxide for the degradation of norfloxacin, Ultrason. Sonochem., 40 (2018) 763–772.
[39] Y.F. Zhang, J.H. Fan, B. Yang, W.T. Huang, L.M. Ma, Copper-catalyzed activation of molecular oxygen for oxidative destruction of acetaminophen: the mechanism and superoxide mediated cycling of copper species, Chemosphere, 166 (2017) 89–95.
[40] S. Jorfi, S. Pourfadakari, M. Ahmadi, H. Akbari, Thermally activated persulfate treatment and mineralization of a recalcitrant high TDS petrochemical wastewater, Pol. J. Chem. Technol., 19 (2017) 72–77.
[41] Z.G. Rahmata, M. Ahmadic, Activation of persulfate by Fe^{2+} for saline recalcitrant petrochemical wastewater treatment: intermediates identification and kinetic study, Desal. Water Treat., 166 (2019) 35–43.
[42] M. Ahmadia, N.J. Haghighifarda, R.D.C. Soltanic, M. Tobeishib, S. Jorfia, Treatment of a saline petrochemical wastewater containing recalcitrant organics using Electro-Fenton process: persulfate and ultrasonic intensification, Desal. Water Treat., 169 (2019) 241–250.
[43] A.H. Hilles, S.S.A. Amr, R.A. Hussein, O.D. El-Sebaie, A.I. Arafa, Performance of combined sodium persulfate/H_2O_2 based advanced oxidation process in stabilized landfill leachate treatment, J. Environ. Manage., 166 (2016) 493–498.
[44] A.R. Ishak, F.S. Hamid, S. Mohamad, K.S. Tay, Stabilized landfill leachate treatment by coagulation-flocculation coupled with UV-based sulfate radical oxidation process, Waste Manage., 76 (2018) 575–581.
[45] C. Chen, H. Feng, Y. Deng, Re-evaluation of sulfate radical based–advanced oxidation processes (SR-AOPs) for treatment of raw municipal landfill leachate, Water Res., 153 (2019) 100–107.
[46] J. Antony, S.V. Niveditha, R. Gandhimathi, S.T. Ramesh, P.V. Nidheesh, Stabilized landfill leachate treatment by zero valent aluminium-acid system combined with hydrogen peroxide and persulfate based advanced oxidation process, Waste Manage., 106 (2020) 1–11.
[47] M.S. Bhatti, D. Kapoor, R.K. Kalia, A.S. Reddy, A.K. Thukral, RSM and ANN modeling for electrocoagulation of copper from simulated waste water: multi objective optimization using genetic algorithm approach, Desalination, 274 (2011) 74–80.
[48] P. Tripathi, V.C. Srivastava, A. Kumar, Optimization of an azo dye batch adsorption parameters using Box–Behnken design, Desalination, 249 (2009) 1273–1279.

[49] R. Gottipati, S. Mishra, Process optimization of adsorption of Cr(VI) on activated carbons prepared from plant precursors by a two-level full factorial design, Chem. Eng. J., 160 (2010) 99–107.
[50] S. Bajpaia, S.K. Guptab, A. Deyc, M.K. Jhaa, V. Bajpaia, S. Joshi, A. Gup, Application of Central Composite Design approach for removal of chromium(VI) from aqueous solution using weakly anionic resin: modeling, optimization and study of interactive variables, J. Hazard. Mater., 227–228 (2012) 436–444.
[51] APHA/AWWA/WEF, Standard Methods for the Examination of Water and Wastewater, 21st ed., American Public Health Association/American Water Works Association/Water Environment Federation, Washington DC, 2005.
[52] S. Singh, J.P. Chakraborty, M.K. Mondal, Optimization of process parameters for torrefaction of *Acacia nilotica* using response surface methodology and characteristics of torrefied biomass as upgraded fuel, Energy, 186 (2019) 115865.
[53] M. Ahmadi, F. Vahabzadeh, B. Bonakdarpour, E. Mofarrah, M. Mehranian, Application of the central composite design and response surface methodology to the advanced treatment of olive oil processing wastewater using Fenton's peroxidation, J. Hazard. Mater., 123 (2005) 187–195.
[54] Q. Beg, V. Sahai, R. Gupta, Statistical media optimization and alkaline protease production from *Bacillus mojavensis* in a bioreactor, Process Biochem., 39 (2003) 203–209.
[55] Y. Rostamiyan, A. Fereidoon, A.H. Mashhadzadeh, M.R. Ashtiyani, A. Salmankhani, Using response surface methodology for modeling and optimizing tensile and impact strength properties of fiber orientated quaternary hybrid nano composite, Composites, Part B, 69 (2015) 304–316.
[56] H. Li, S. Zhou, Y. Sun, J. Lv, Application of response surface methodology to the advanced treatment of biologically stabilized landfill leachate using Fenton's reagent, Waste Manage., 30 (2010) 2122–2129.
[57] A.A.L. Zinatizadeh, A.R. Mohamed, A.Z. Abdullah, M.D. Mashitah, I.M. Hasnain, G.D. Najafpour, Process modeling and analysis of palm oil mill effluent treatment in an up-flow anaerobic sludge mixed film bioreactor using response surface methodology (RSM), Water Res., 40 (2006) 3193–3208.
[58] F. Görmez, Ö. Görmez, E. Yabalak, B. Gözmen, Application of the central composite design to mineralization of olive mill wastewater by the electro/FeII/persulfate oxidation method, SN Appl. Sci., 2 (2020) 178.
[59] B. Gozmen, O. Sonmez, M. Turabik, Response surface methodology for oxidative degradation of the basic yellow 28 dye by temperature and ferrous ion activated persulfate, Asian J. Chem., 25 (2013) 6831–6839.
[60] T.F. Awolusi, O.L. Oke, O.O. Akinkurolere, A.O. Sojobi, Application of response surface methodology: predicting and optimizing the properties of concrete containing steel fibre extracted from waste tires with limestone powder as filler, Case Stud. Constr. Mater., 10 (2019) e00212.
[61] A. Babuponnusami, K. Muthukumar, Removal of phenol by heterogenous photo electro Fenton-like process using nano-zero valent iron, Sep. Purif. Technol., 98 (2021) 130–135.
[62] S. Zha, Y. Cheng, Y. Gao, Z. Chen, M. Megharaj, R. Naidu, Nanoscale zero-valent iron as a catalyst for heterogeneous Fenton oxidation of amoxicillin, Chem. Eng. J., 255 (2014) 141–148.
[63] A.A. Burbano, D.D. Dionysiou, M.T. Suidan, T.L. Richardson, Oxidation kinetics and effect of pH on the degradation of MTBE with Fenton reagent, Water Res., 39 (2005) 107–118.
[64] Y. Wang, W. Chu, Photo-assisted degradation of 2, 4, 5-trichlorophenoxyacetic acid by Fe (II)-catalyzed activation of Oxone process: the role of UV irradiation, reaction mechanism and mineralization, Appl. Catal. B: Environ., 123 (2012) 151–161.
[65] B.Z. Li, L. Li, K.F. Lin, W. Zhang, S.G. Lu, Q.S. Luo, Removal of 1,1,1-trichloroethane from aqueous solution by a sono-activated persulfate process, Ultrason. Sonochem., 20 (2013) 855–863.
[66] C. Cai, H. Zhang, X. Zhong, L.W. Hou, Electrochemical enhanced heterogeneous activation of peroxydisulfate by Fe-Co/SBA-15 catalyst for the degradation of Orange II in water, Water Res., 66 (2014) 473–485.
[67] T. Zhang, Y. Yang, X. Li, H. Yu, N. Wang, H. Li, P. Du, Y. Jiang, X. Fan, Z. Zhou, Degradation of sulfamethazine by persulfate activated with nanosized zerovalent copper in combination with ultrasonic irradiation, Sep. Purif. Technol., 239 (2020) 116537.
[68] F. Ghanbari, M. Moradi, M. Manshouri, Textile wastewater decolorization by zero valent iron activated peroxymonosulfate: compared with zero valent copper, J. Environ. Chem. Eng., 2 (2014) 1846–1851.
[69] A.A. Babaei, F. Ghanbari, COD removal from petrochemical wastewater by UV/hydrogen peroxide, UV/persulfate and UV/percarbonate: biodegradability improvement and cost evaluation, J. Water Reuse Desal., 6 (2016) 484–494.
[70] A.R. Zarei, H. Rezaeivahidian, A.R. Soleymani, Mineralization of unsymmetrical dimethylhydrazine (UDMH) via persulfate activated by zero valent iron nano particles: modeling, optimization and cost estimation, Desal. Water Treat., 57 (2016) 16119–16128.
[71] Y.C. Chou, S.L. Lo, J. Kuo, C.J. Yeh, Microwave-enhanced persulfate oxidation to treat mature landfill leachate, J. Hazard. Mater., 284 (2015) 83–91.
[72] A.R. Soleymani, M. Moradi, Performance and modeling of UV/persulfate/Ce(IV) process as a dual oxidant photochemical treatment system: kinetic study and operating cost estimation, Chem. Eng. J., 347 (2018) 243–251.
[73] N. Genç, E. Durna, H.K. Kayapinar Cicigün, Response Surface Modeling and Optimization of Microwave-Activated Persulfate Oxidation of Olive Oil Mill Wastewater, CLEAN–Soil Air Water, 48 (2020) 1900198.
[74] G. Varank, S. Yazici Guvenc, K. Dincer, A. Demir, Concentrated Leachate Treatment by Electro-Fenton and Electro-Persulfate Processes Using Central Composite Design, Int. J. Environ. Res., 14 (2020) 439–461.
[75] N. Genç, E. Durna, Simultaneous optimization of treatment efficiency and operating cost in leachate concentrate degradation by thermal-activated persulfate catalysed with Ag (I): comparison of microwave and conventional heating, J. Microwave Power Electromagn. Energy, 53 (2019) 155–170.
[76] A.H. Hilles, S.S.A. Amr, R.A. Hussein, A.I. Arafa, O.D. El-Sebaie, Effect of persulfate and persulfate/H_2O_2 on biodegradability of an anaerobic stabilized landfill leachate, Waste Manage., 44 (2015) 172–177.
[77] B.K. Tripathy, M. Kumar, Sequential coagulation/flocculation and microwave-persulfate processes for landfill leachate treatment: assessment of bio-toxicity, effect of pretreatment and cost-analysis, Waste Manage., 85 (2019) 18–29.